the cells with leptin for 1 to 2 hours before addition of insulin partially reversed the down-regulating effect of insulin on PEPCK expression (Fig. 5). This observation is in contrast with the leptin-induced increase in PI 3-kinase activity obtained in HepG2 cells. Furthermore, the kinetics of the effect of leptin on PEPCK expression excludes its possible mediation by GRB2. It is therefore likely that leptin affects PEPCK gene expression by an as yet unknown pathway. On the basis of these results, we propose that leptin may affect gluconeogenesis, at least in the H4-II-E cell line, by attenuating the effect of insulin on the expression of PEPCK.

Several mouse strains that are deficient in leptin or OB-R serve as models for obesity, insulin resistance, and non-insulin–dependent diabetes mellitus (*1*, *4*, *14*). Therefore, it appears that excess leptin, as well as a complete absence of leptin, may impair some insulin responses, although not necessarily by the same mechanism. In the absence of leptin, other obesity-related factors may attenuate insulin responses. One such factor is TNF-α, which is overexpressed in adipocytes of obese animals. TNF-α down-regulates insulin-induced phosphorylation of IRS-1 and reduces expression of the insulin-dependent glucose transporter Glut4 (*10*, *15*).

Tyrosine phosphorylation of IRS-1 by the IR kinase is a key step in the IR signaling cascade, and GRB2 further mediates parts of this cascade (*8*, *16*). Therefore, the leptin-induced dephosphorylation of IRS-1 and its dissociation from GRB2 indicate that leptin may antagonize some functions of insulin. Although insulin resistance is poorly understood, it probably results from a combination of several factors and processes. Our finding that leptin attenuates some insulin-induced signals in hepatic cell lines, and the reports of increased serum leptin in obesity, warrants further studies on the possible role of leptin in obesity-associated insulin resistance.

REFERENCES AND NOTES

1. Y. Zhang *et al.*, *Nature* **372**, 425 (1994).
2. M. A. Pelleymounter *et al.*, *Science* **269**, 540 (1995); J. L. Halaas *et al.*, *ibid.*, p. 543; L. A. Campfield, F. J. Smith, Y. Guisez, R. Devos, P. Burn, *ibid.*, p. 546; D. S. Weigle *et al.*, *J. Clin. Invest.* **96**, 2065 (1995); S. Collins *et al.*, *Nature* **380**, 677 (1996).
3. L. A. Tartaglia *et al.*, *Cell* **83**, 1263 (1995).
4. G. H. Lee *et al.*, *Nature* **379**, 632 (1996).
5. J. A. Cioffi *et al.*, *Nature Med.* **2**, 585 (1996).
6. F. Lonnqvist, P. Arner, L. Nordfors, M. Schalling, *ibid.* **1**, 950 (1995); M. Maffei *et al.*, *ibid.*, p. 1155; R. C. Frederich *et al.*, *ibid.*, p. 1311; R. V. Considine *et al.*, *N. Engl. J. Med.* **334**, 292 (1996).
7. J. P. Felber and A. Golay, *Metabolism* **44** (suppl. 2), 4 (1995).
8. B. Cheatham and C. R. Kahn, *Endocrinol. Rev.* **16**, 117 (1995).
9. X. J. Sun, D. L. Crimmins, M. G. Myers Jr., M. Miralpeix, M. F. White, *Mol. Cell. Biol.* **13**, 7418 (1993); E. Y. Skolnik *et al.*, *EMBO J.* **12**, 1929 (1993).
10. G. S. Hotamisligil *et al.*, *Science* **271**, 665 (1996).
11. M. G. Myers Jr. *et al.*, *Endocrinology* **132**, 1421 (1993).
12. T. G. Yin, M. L. S. Tsang, Y. C. Yang, *J. Biol. Chem.* **269**, 26614 (1994); T. G. Yin *et al.*, *ibid.* **270**, 20497 (1995); S. Uddin *et al.*, *ibid.*, p. 15938; A. Pernis *et al.*, *Proc. Natl. Acad. Sci. U.S.A.* **92**, 7971 (1995).
13. D. Granner, T. Andreone, K. Sasaki, E. Beale, *Nature* **305**, 549 (1983); L. Xing and P. G. Quinn, *Mol. Endocrinol.* **7**, 1484 (1993).
14. H. Chen *et al.*, *Cell* **84**, 491 (1996); S. C. Chua Jr. *et al.*, *Science* **271**, 994 (1996).
15. R. Feinstein, H. Kanety, M. Z. Papa, B. Lunenfeld, A. Karasik, *J. Biol. Chem.* **268**, 26055 (1993); G. S. Hotamisligil, A. Budavari, D. Murray, B. M. Spiegelman, *J. Clin. Invest.* **94**, 1543 (1994); G. S. Hotamisligil and B. M. Spiegelman, *Diabetes* **43**, 1271 (1994); H. Kanety, R. Feinstein, M. Z. Papa, R. Hemi, A. Karasik, *J. Biol. Chem.* **270**, 23780 (1995).
16. M. G. Myers Jr. and M. F. White, *Diabetes* **42**, 643 (1993); M. G. Myers Jr., X. J. Sun, M. F. White, *Trends Biochem. Sci.* **19**, 289 (1994); M. G. Myers Jr. *et al.*, *Mol. Cell. Biol.* **14**, 3577 (1994); D. W. Rose, A. R. Saltiel, M. Majumdar, S. J. Decker, J. M. Olefsky, *Proc. Natl. Acad. Sci. U.S.A.* **91**, 797 (1994); H. Tamemoto *et al.*, *Nature* **372**, 182 (1994); E. Araki *et al.*, *ibid.*, p. 186; M. F. White and C. R. Kahn, *J. Biol. Chem.* **269**, 1 (1994).
17. Mouse leptin was purchased from Peprotech (Princeton, NJ). Antiserum to mouse leptin was obtained from a rabbit. For details on radioiodination, cross-linking, saturation binding, and Scatchard analysis, see B. Cohen, D. Novick, S. Barak, M. Rubinstein, *Mol. Cell. Biol.* **15**, 4208 (1995).
18. Serum-starved (24 hours) cells (4×10^7 cells) in Eagle's minimal essential medium were treated with insulin and leptin as indicated. Cells were washed three times with cold phosphate-buffered saline containing 1 mM Na_3VO_4 and lysed with 1 ml of cold lysis buffer [50 mM tris-HCl (pH 8.0), 1% Triton X-100, 1 mM Na_2 EDTA, 1 mM $MgCl_2$, 100 mM NaF, 1 mM phenylmethanesulfonyl fluoride, and aprotinin (5 μg/ml)]. Immunoprecipitation or precipitation with GST-GRB2 fusion protein was done on the clarified lysates. All autoradiograms were quantitated by densitometry and are averages of three independent experiments.
19. A. Kosaki, T. S. Pillay, L. Xu, N. J. Webster, *J. Biol. Chem.* **270**, 20816 (1995).
20. A. Ando *et al.*, *EMBO J.* **13**, 3033 (1994).

21. We thank S. Barak for technical help; H. S. Kim for help in Northern blot analysis; Y. Groner for valuable discussions; Y. Zick and H. Kanety for advice and for antibodies to IRS-1 and IR; Y. Yarden and G. Levkowitz for GST-GRB2 fusion protein; M. Walker, Y. Schechter, and D. Wallach for reviewing the manuscript; and M. Spigel for editorial assistance. M.R. holds the Edna and Maurice Weiss Chair of cytokine research.

19 July 1996; accepted 27 September 1996

From Peptide Precursors to Oxazole and Thiazole-Containing Peptide Antibiotics: Microcin B17 Synthase

Yue-Ming Li, Jill C. Milne, Lara L. Madison, Roberto Kolter, Christopher T. Walsh*

Escherichia coli microcin B17 is a posttranslationally modified peptide that inhibits bacterial DNA gyrase. It contains four oxazole and four thiazole rings and is representative of a broad class of pharmaceutically important natural products with five-membered heterocycles derived from peptide precursors. An in vitro assay was developed to detect heterocycle formation, and an enzyme complex, microcin B17 synthase, was purified and found to contain three proteins, McbB, McbC, and McbD, that convert 14 residues into the eight mono- and bisheterocyclic moieties in vitro that confer antibiotic activity on mature microcin B17. These enzymatic reactions alter the peptide backbone connectivity. The propeptide region of premicrocin is the major recognition determinant for binding and downstream heterocycle formation by microcin B17 synthase. A general pathway for the enzymatic biosynthesis of these heterocycles is formulated.

A growing number of peptide-based natural products have been found to contain thiazole and oxazole heterocyclic rings and exhibit significant antifungal, antibiotic, antitumor, and antiviral biological activities (*1*). The five molecules depicted in Fig. 1, bleomycin A_2, thiangazole, patellamide A, pristinamycin II_A, and thiostrepton, exemplify the patterns of such heterocycle occurrence in molecules of therapeutic interest. The antitumor antibiotic bleomycin uses the bithiazole moiety to intercalate into DNA (*2*). The tandem four-ring structure of thiangazole including the β-methyloxazoline provides potent antiviral activity against human immunodeficiency virus (*3*). Patellamides, cyclic octapeptides of marine origin, have antitumor properties (*4*). Thiostrepton, a protein synthesis inhibitor with four thiazole and one thiazoline ring is a signature secondary metabolite of *Streptomycetes* (*5*). Derivatives of pristinamycin (for example, RP59500) are currently in advanced clinical testing for combating vancomycin-resistant Gram-positive bacterial infections (*6*). The heterocyclic rings are likely to arise by cyclization of

Y.-M. Li, J. C. Milne, C. T. Walsh, Department of Biological Chemistry and Molecular Pharmacology, Harvard Medical School, Boston, MA 02115, USA.
L. L. Madison and R. Kolter, Department of Microbiology and Molecular Genetics, Harvard Medical School, Boston, MA 02115, USA.

*To whom correspondence should be addressed.

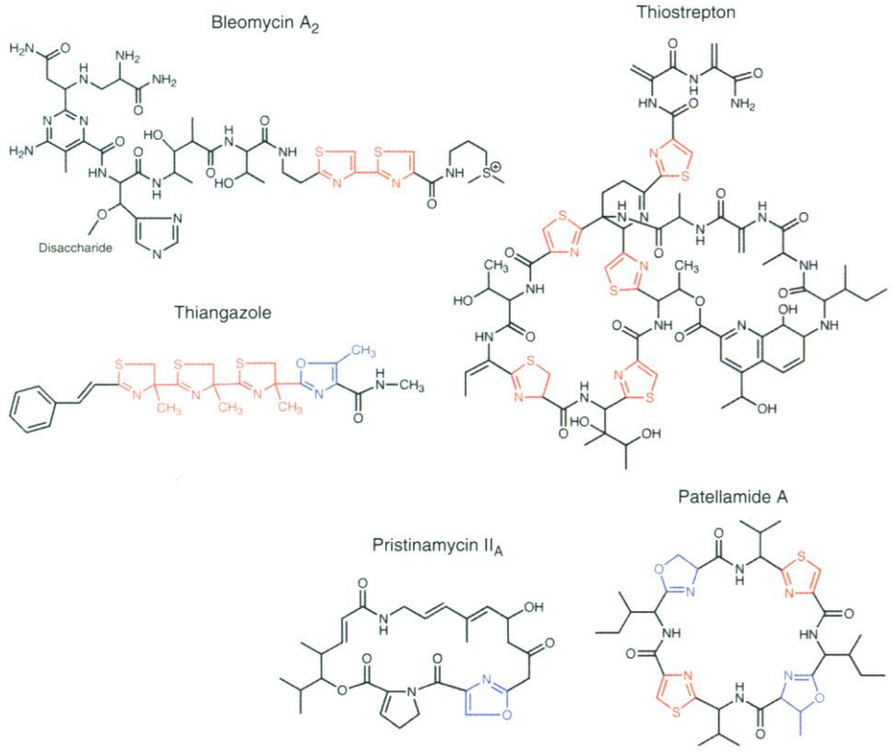

Fig. 1. Structures of bleomycin A_2, thiostrepton, thiangazole, pristinamycin II_A, and patellamide A. Thiazoline (dihydrothiazole) and thiazole rings are shown in red and oxazoline (dihydrooxazole) and oxazole rings are shown in blue.

peptide precursors; for example, a -Gly-Cys- dipeptide sequence converted to an aminomethylthiazoline, then modified to the aminomethylthiazole, and analogously, -Gly-Ser-converted to aminomethyloxazoline and modified to aminomethyloxazole.

Until recently little was known about the molecular genetics or the enzymology of thiazole and oxazole ring biogenesis. The *E. coli* peptide antibiotic microcin B17 (MccB17), which represents a class of DNA gyrase inhibitors (*7*) distinct from quinolone or coumarin drugs, contains four thiazoles and four oxazoles fashioned from six glycines, four cysteines, and four serines present in pre-MccB17 (Fig. 2) (*8*). These initial studies of MccB17 have provided both the genetic and biochemical opportunity to begin decoding the molecular logic for the construction of both isolated oxazole and thiazole rings and the 4,2-bisheterocycles because the tripeptide sequences $Gly^{39}Ser^{40}Cys^{41}$ and $Gly^{54}Cys^{55}Ser^{56}$ in pre-MccB17 yield a 4,2-linked oxazole-thiazole and a 4,2-thiazole-oxazole, respectively. Analogous to bleomycin, each of the bisheterocyles could be intercalation moieties involved in the DNA gyrase inhibition that leads to accumulation of the cleaved DNA intermediate (*7*).

The *E. coli* MccB17 operon has been characterized by genetic analysis and provisional roles assigned to seven open reading frames, *mcbA*, *-B*, *-C*, *-D*, *-E*, *-F*, and -G. The gene *mcbA* encodes the 69–amino acid (aa) pre-MccB17 polypeptide. Three genes, *mcbB*, *-C*, and *-D*, are required for the conversion of nascent pre-MccB17 to pro-MccB17 (Fig. 2) (*9*, *13*). The first 26 amino acids of pro-MccB17 are removed proteolytically to yield the active antibiotic (*11*, *14*), MccB17 (residues 27 through 69), that is transported out of the producing *E. coli* cell by McbE and McbF (*12*). MccB17 is then taken up by susceptible cells where gyrase is the killing target (*7*). A seventh gene, *mcbG*, provides immunity to the MccB17-producing strain (*12*).

Purification and characterization of active MccB17 synthase complex required the availability of substrates and a specific assay for detection of cyclized products from acyclic peptide precursors. Prior pulse-chase studies on the expression and lifetime of pre-MccB17 revealed very rapid degradation (*15*), not unanticipated given the high glycine content including 11 out of 12 residues at positions 28 through 39 in the McbA nascent product (Fig. 2). We prepared three substrates (Fig. 3A): (i) the first 65 codons of *mcbA* were fused to β-galactosidase, creating a fusion protein of 102 kD, McbA–β-Gal, which has been useful for both in vitro and in vivo studies (*15*); (ii) an NH_2-terminal hexa-histidine tag was fused in frame to *mcbA*, yielding His_6-McbA (*16*), which could be overproduced and affinity purified from *E. coli* cell extracts by Ni^{2+}-chelate chromatography; and (iii) a fragment con-

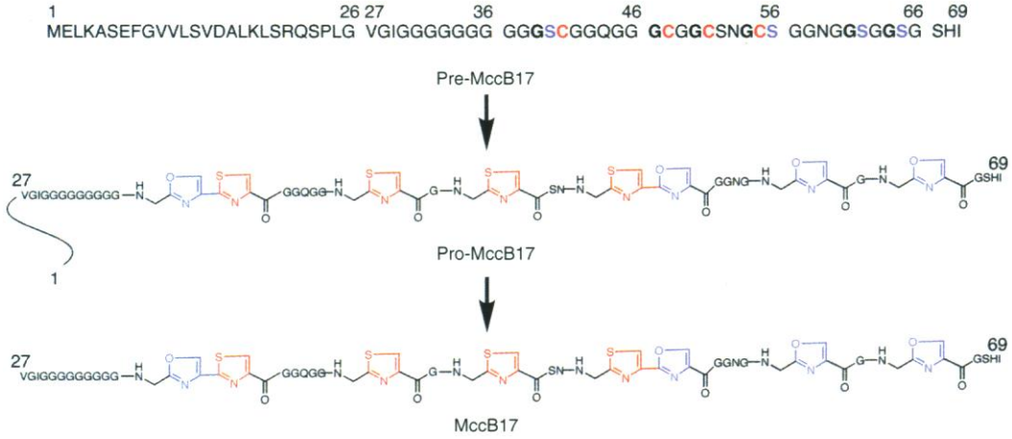

Fig. 2. Structure of microcin B17 (MccB17) and its maturation pathway. MccB17 contains four thiazole (red) and four oxazole (blue) rings that are derived from the posttranslational modification of Cys (red) and Ser (blue) residues, respectively. The *mcbA* gene encodes a 69–amino acid precursor (pre-MccB17) that undergoes at least two steps of posttranslational modification. First, the products of the genes *mcbB*, *-C*, and *-D* mediate heterocycle formation to generate pro-MccB17. Subsequently, the NH_2-terminal 26 residues are removed, yielding mature MccB17. The Met residue at the NH_2-terminus of pre-MccB17 was designated as the first residue in the numbering scheme used in this study. Abbreviations for the amino acid residues are as follows: A, Ala; C, Cys; D, Asp; E, Glu; F, Phe; G, Gly; H, His; I, Ile; K, Lys; L, Leu; M, Met; N, Asn; P, Pro; Q, Gln; R, Arg; S, Ser; T, Thr; V, Val; W, Trp; and Y, Tyr.

taining the first 46 residues of McbA [McbA(1–46)] was synthesized, which included the putative 26-aa propeptide or leader sequence and the $Gly^{39}Ser^{40}Cys^{41}$ tripeptide sequence that is a locus for bisheterocycle formation in MccB17 posttranslational maturation.

To assay these potential substrates we used a polyclonal antibody that recognizes mature MccB17 and pro-MccB17, but not pre-MccB17 (Fig. 2) (*14*), which we reasoned to indicate that this antibody recognized one or more heterocycles as determinants, which was later validated. We further determined that this antibody recognizes the bithiazole fragment used in the synthesis of bleomycin when it is conjugated to bovine serum albumin (BSA) (*17*). When each of the three substrates was incubated with an *E. coli* extract containing McbB, -C, and -D, a linear signal was detected by protein immunoblot analysis with antibodies to MccB17 (anti-MccB17). Data for the McbA–β-Gal substrate is shown in Fig. 3B. The enzymatic activity monitored by immunoblot required the presence of each of the three proteins McbB, McbC, and McbD, as assessed by an in vitro assay with knockout strains (*mcbB*$^-$, *mcbC*$^-$, and *mcbD*$^-$) (*18*, *19*).

Purification of MccB17 synthase from the antibiotic-producing strain ZK4(pPY113) (*14*, *20*) resulted in a 59-fold increase in specific activity (*21*). Starting from 3.6 g of *E. coli* soluble protein, we obtained 9.5 mg of the purified protein with an overall yield of 16%. Purified MccB17 synthase has a Michaelis constant K_m of 2.3 μM for McbA(1–46) and an estimated catalysis constant k_{cat} of 0.2 min^{-1}, on the basis of formation of both heterocyclic rings (*22*).

SDS-PAGE analysis of purified MccB17 synthase revealed three major protein bands at apparent molecular sizes of 68, 45, and 31 kD (Fig. 4A). NH_2-terminal sequencing and protein immunoblot analysis demonstrated that the 31-kD band contained two proteins, McbB (33 kD) and McbC (31 kD), and the 45-kD band was McbD. The NH_2-terminal sequence of the purified proteins showed that (i) McbB was translated from the second potential start site rather than the first one (*13*), (ii) the first Met was removed in McbC, and (iii) the open reading frames for *mcbC* and *mcbD* overlap by 20 bases (*13*). The fourth protein, at ~68 kD, had the sequence of HtpG, an *E. coli* member of the Hsp90 heat shock protein family (*23*).

In a parallel set of experiments we separately overproduced McbB, His_6-McbC, and His_6-McbD (*24*), purified each to homogeneity, and raised monospecific polyclonal antibodies with no cross-reactivity to each other. We used these three antibodies to confirm that McbB, -C, and -D make up a MccB17 synthase complex by immunoprecipitating them from crude extracts of *E. coli* ZK4(pPY113). McbB is co-precipitated with McbC and McbD by anti-McbC or

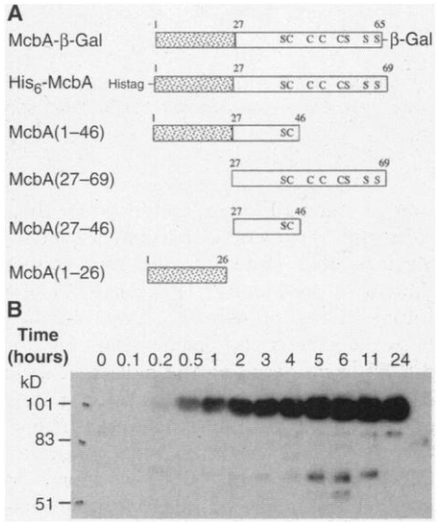

Fig. 3. (**A**) Representation of fusion proteins and peptides used as substrates or inhibitors of MccB17 synthase; C (Cys) and S (Ser) represent the residues that are posttranslationally modified to form the heterocycles; thus, McbA(1–46) has two modifiable residues and McbA(1–26) has none. McbA–β-Gal was produced and purified as described (*42*). McbA(1–46), -(27–69), -(27–46), and -(1–26) were synthesized with a solid-phase synthetic strategy (*43*). The stippled region represents the propeptide sequence. (**B**) Time dependence of McbA–β-Gal modification by MccB17. synthase. The reaction mixture contained 150 μM McbA–β-Gal, 50 mM tris-HCl (pH 7.5), 50 mM KCl, 2 mM $MgCl_2$, 1 mM $CaCl_2$, 1 mM adenosine triphosphate (ATP), 1 mM dithiothreitol (DTT), and cellular protein (3.5 mg/ml) [supernatant of a lysate from ZK4(pPY113) centrifuged at 15,000*g*]. The reaction was carried out at 37°C and stopped by adding SDS–polyacrylamide gel electrophoresis (PAGE) sample buffer. Samples were analyzed by SDS-PAGE (7.5% polyacrylamide) followed by protein immunoblot analysis. The primary antibody was a polyclonal antibody specific for pro- and mature MccB17 (*14*), and the secondary antibody was goat antibody to rabbit immunoglobulin (horseradish peroxidase conjugate) (Pierce). The protein immunoblot was developed with the SuperSignal reagent (Pierce).

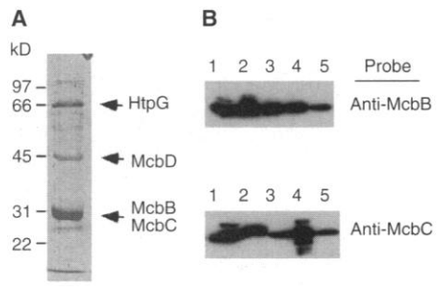

Fig. 4. (**A**) Purified MccB17 synthase. MccB17 synthase was purified as described (*44*). (**B**) Co-immunoprecipitation of McbB, -C, and -D. The immunoprecipitates were probed with anti-McbB or anti-McbC. Lane 1, soluble fraction of ZK4(pPY113) before immunoprecipitation; lane 2, purified protein (McbB, upper panel and His_6-McbC, lower panel); lane 3, ZK4(pPY113) lysate precipitated with anti-McbB; lane 4, ZK4(pPY113) lysate precipitated with anti-McbC; and lane 5, ZK4(pPY113) lysate precipitated by anti-McbD. The three proteins McbB, His_6-McbC, and His_6-McbD, were individually overexpressed, purified to homogeneity (*24*), and used for antibody production (*45*). The soluble fraction (105,000*g* supernatant) of ZK4(pPY113) was separately incubated with anti-McbB (1:50 dilution), anti-McbC (1:100), and anti-McbD (1:25) at 4°C for 2 hours; then protein A–Sepharose (Pharmacia) was added and the mixture incubated for 1 hour (*45*).

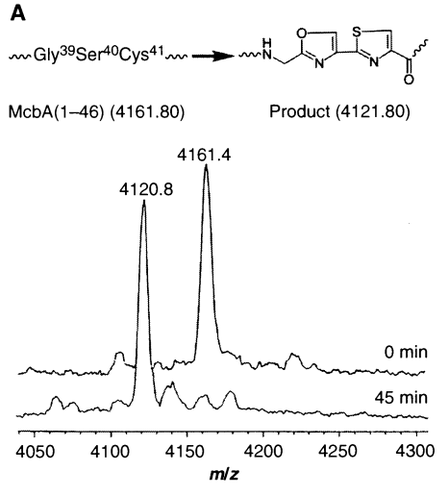

B

Substrate	Substrate		Product	
	Calc.	Meas.	Calc.	Meas.
McbA(1–46)	4161.80	4160.40	4121.80	4119.80
His_6-McbA	8046.40	8058.30	7886.40	7888.10

Fig. 5. (**A**) MS analysis ($[M + H]^+$) of the HPLC-purified products of MccB17 synthase action after 0 min and 45 min (*46*). The peaks (33% solvent B) from the 0- and 45-min reactions represent the starting material [McbA(1–46)] and the final product [Mcb(1–46) containing the 4,2-oxazole-thiazole moiety], respectively (*18*). (**B**) Summary of the MS analysis of substrates McbA(1–46) and His_6-McbA. The reactions with His_6-McbA as substrate were carried out as described above for Mcb(1–46) except that the time points analyzed were 0 and 60 min. His_6-McbA eluted from HPLC at 30% solvent B. As with Mcb(1–46), MS analysis of the HPLC peaks for the 0- and 60-min reactions indicate that the peaks represent the starting material and the final product (His_6-McbA containing four oxazoles and four thiazoles), respectively. Calc., calculated mass; Meas., measured mass.

anti-McbD (Fig. 4B). McbC is co-precipitated by anti-McbB and anti-McbD. McbD is not well resolved from the immunoglobulin G bands in such immunoprecipitates. We do not yet know the stoichiometry of McbB, -C, and -D in the active MccB17 synthase complex, although enzyme activity migrates on a size-exclusion column with an apparent molecular size of ~100 kD, minimally consistent with unitary stoichiometry of McbB (33 kD), McbC (31 kD), and McbD (45 kD).

Given that the activity assay to this point relied on formation of antibody-positive material, we sought to define the nature of the enzymatic modification more precisely. We turned to both the His_6-McbA construct with eight potential sites for heterocycle formation and McbA(1–46), which contains two modifiable residues Ser^{40} and Cys^{41}, but no others. Both peptides were substrates in the anti-MccB17 protein immunoblot assays as described above, but the question arose as to how many modifications were being introduced in vitro by purified MccB17 synthase. Purified MccB17 synthase was incubated with McbA(1–46) for 45 min, then subjected to high-performance liquid chromatography (HPLC). The product of the McbA(1–46) peak was recognized by anti-MccB17. Mass spectrometric (MS) analysis revealed that the mass of the starting material was 4160.4 [calculated mass for McbA(1–46), 4161.8], and the mass of the antibody-positive material was 4119.8 (Fig. 5). The 4120 peak was absent from the controls at zero time or if MccB17 synthase was omitted from the incubation mix. Conversion of the $Gly^{39}Ser^{40}Cys^{41}$ tripeptide moiety into the 4,2-oxazole-thiazole resulted in the loss of 40 mass units for a calculated mass of 4121.8, very close to the observed 4119.8 (Fig. 5). Two points are thus established. First, anti-MccB17 recognizes heterocycle-containing product, and second, the tandem bisheterocycle is made from McbA(1–46), with no accumulation of either the monocyclic thiazole or oxazole intermediate (calculated mass of 4142) at the time point examined. The His_6-McbA construct has all the eight possible sites of heterocycle modification for a total decrease in mass of $8 \times 20 = 160$ mass units if all sites are recognized. In the event, incubation of His_6-McbA with purified enzyme complex, followed by HPLC and initial localization of the product by protein immunoblot analysis, gave fractions with mass of 7888.10 (calculated mass of fully modified product = 7886.40), whereas the starting material (His_6-McbA) in the absence of enzyme or in the time zero sample gave 8058.30 (calculated = 8046.4), for a loss of 170 mass units. These data demonstrate that purified MccB17 synthase is able to convert four serines and four cysteines in premicrocin (McbA) to the full complement of heterocycles found in the antibiotic.

Given the effective processing of McbA(1–46) by purified MccB17 synthase, we prepared the fragment McbA(27–69) (Fig. 3A) that contains the 43 aa that end up in the mature, posttranslationally processed MccB17 antibiotic. In contrast to the McbA(1–46) substrate behavior, we could detect no enzymatic conversion of McbA(27–69) over a concentration range of 2 to 140 μM, under conditions where we could easily have detected 5% of the signal produced with McbA(1–46). We estimate by k_{cat}/K_m (catalytic efficiency) that the 43-aa fragment, McbA(27–69), is at least 500- to 1000-fold less efficient than McbA(1–46). Next, we assessed the ability of McbA(27–69) and also a peptide composed of residues 27 through 46 [McbA(27–46)] to block processing of McbA(1–46) and observed no inhibition at 80 μM McbA(27–69) or McbA(27–46). In contrast, the 26-aa propeptide, McbA(1–26), inhibited modification of McbA(1–46) with an IC_{50} (median inhibitory concentration) of 2 μM, essentially the same as the K_m for McbA(1–46) (25). Taken together, these results indicate that most if not all of the recognition of substrate by MccB17 synthase is provided by the leader or propeptide region. This is reminiscent of the eukaryotic vitamin K–dependent carboxylase posttranslational modification of the first 10 to 12 glutamyl residues to γ-carboxyglutamates in such zymogens as factor IX, factor X, and prothrombin (26). In these proteins an 18-residue propeptide region, the γ-carboxylase recognition sequence, also provides a 1000-fold increase in affinity for downstream modification of peptide substrates. Recent data concerning the nisin family of lanthionine polypeptide antibiotics also indicate interaction of the propeptide region with a multimeric lanthionine synthetase complex (27). By analogy, one or more of the McbB, -C, or -D subunits may recognize the propeptide(1–26) region before downstream heterocycle formation (28).

An initial survey of potential cofactor requirements for MccB17 synthase–mediated conversion of Ser and Cys residues into oxazole and thiazole rings was conducted with the McbA–β-Gal fusion protein as a substrate. One requirement, apparent from the protein immunoblot assay, was adenosine triphosphate (ATP), which has a K_m of 89

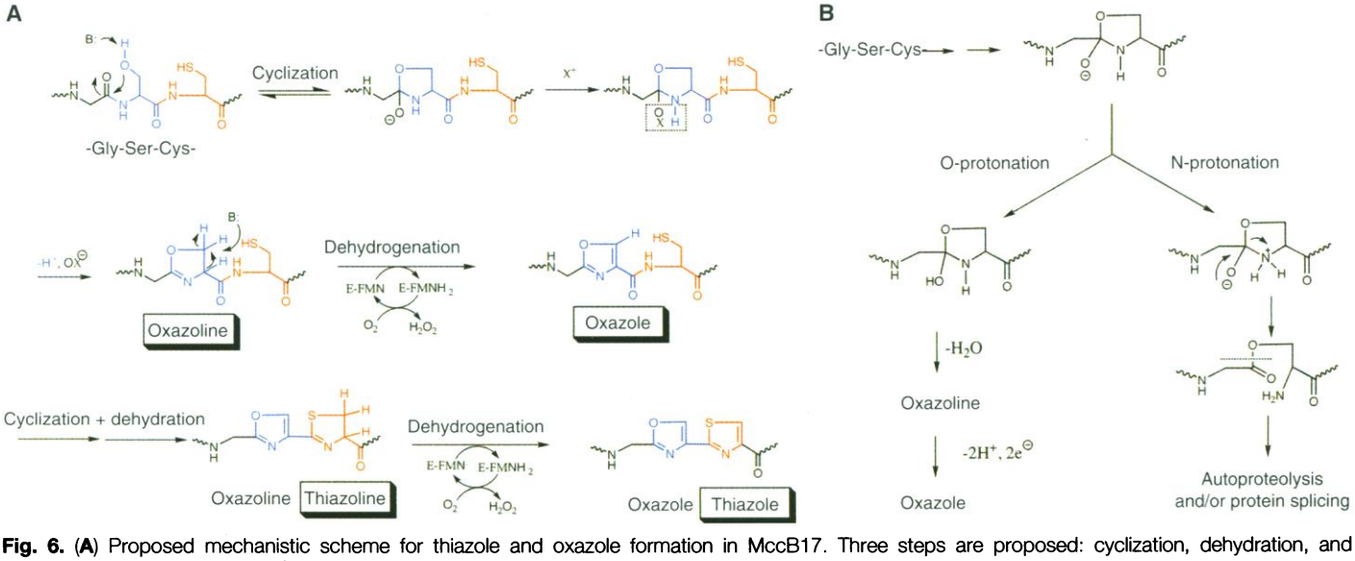

Fig. 6. (**A**) Proposed mechanistic scheme for thiazole and oxazole formation in MccB17. Three steps are proposed: cyclization, dehydration, and dehydrogenation. (**B**) Common pathway of heterocycle formation and protein splicing and protein autoproteolysis.

μM. Guanosine triphosphate (GTP) has a K_m of 52 μM, but with one-third the k_{cat}. Adenosine-5′-(γ-thio)triphosphate (ATP-γ-S) could also serve as a substrate, but at a K_m (141 μM) 1.6 times that of ATP and with a 76-fold lower relative k_{cat}, for a 122/1 ratio of ATP/ATP-γ-S by k_{cat}/K_m catalytic efficiency criterion. The ATP analog adenosine diphosphate–CH_2-PO_3^- (AMP-PCP) is a competitive inhibitor, with an inhibitory constant K_i of 2.3 μM. Analysis with [γ-^{32}P]ATP or [α-^{32}P]ATP revealed only adenosine diphosphate and inorganic phosphate (P_i) as products. As yet, we cannot report ATP and heterocycle stoichiometry because of some contaminant peptide-independent adenosine triphosphatase activity.

For each serine or cysteine converted to a heteroaromatic five-membered ring product oxazole or thiazole, two electrons are removed. This redox stoichiometry requirement prompted us to look both for an external electron acceptor and for some redox-active cofactor in the MccB17 synthase complex. One possibility was that nicotinamide adenine dinucleotide (NAD^+) or NAD phosphate ($NADP^+$) might serve as an electron acceptor in the step converting thiazolines to thiazoles or oxazolines to oxazoles (Fig. 6A). However, addition of NAD^+ or $NADP^+$ to the reaction mixture with purified MccB17 synthase had no effect on the rate of product formation (*18*). The most likely terminal electron acceptor then was O_2. Incubations conducted on degassed assay components yielded a reduction in the rate of protein immunoblot–positive product by 2.1-fold for McbA(1–46) under conditions where a glucose–glucose oxidase test system had initial velocity reduced three- to fivefold (*29*). MS analysis on the McbA(1–46) assay revealed no discernible difference between the product produced at lowered O_2 pressure as compared with normal assay conditions. More stringent anaerobiosis will be required to determine a K_m for O_2 and to test whether any oxazoline and thiazoline species form under these conditions.

Although sequence analysis of McbB, -C, and -D failed to detect any signature motifs for cofactors (including for ATP or GTP), it seemed likely that one or more of McbB, -C, or -D should contain a bound redox-active metal or conjugated organic coenzyme to facilitate two-electron oxidation of the proposed thiazoline and oxazoline intermediates (Fig. 6A). Indeed, overproduced and purified McbC was yellow and contained a stoichiometric amount of tightly but noncovalently bound FMN (*18*, *30*).

The detection and purification of MccB17 synthase opens the door for future deconvolution of several aspects of how five-membered ring heterocycles are fashioned enzymically from acyclic peptide precursors, including propeptide recognition, regioselectivity, processivity, minimal size, and number of heterocycles for DNA gyrase inhibition and antibiotic activity. At this point, given our results that reveal elements of the molecular logic for serine-to-oxazole and cysteine-to-thiazole conversions, the mechanistic scheme proposed in Fig. 6A delineates how the $Gly^{34}Ser^{40}Cys^{41}$ tripeptide moiety of MccB17, and specifically in McbA(1–46), is converted to the aminomethyl bisheterocyclic 4,2-oxazole-thiazole, a likely DNA intercalator for subsequent interaction with a DNA-DNA gyrase complex. In both serine-to-oxazole and cysteine-to-thiazole transformation for MccB17, and most likely for all such peptide-derived natural products (for example, Fig. 1), we propose a three-step sequence of cyclization, net dehydration, and subsequent two-electron dehydrogenation.

It is tempting, given three proteins, McbB, -C, and -D, as necessary constituents in MccB17 synthase action, to assign each protein one of these three enzymatic functions, but that would be premature. The cyclization is itself remarkable in likely geometric requirements, and it is reasonable that Gly-Ser and Gly-Cys sequences are favored for cyclization both for lack of steric bulk in the α-CH_2 group of the Gly residue and the Ramachandran angles populated by Gly-X dipeptides. The initial cyclic adduct is likely to be disfavored compared with the acyclic ground state unless the oxyanion formed from the Gly-Ser carbonyl oxygen can be diverted. An obvious route would be enzyme-assisted protonation ($X^+ = H^+$; Fig. 6A). A subsequent dehydration would yield the oxazoline, now more committed to the heterocyclic fate. It is conceivable that X^+ is the γ-PO_3^- from ATP, to yield a phosphate group as –OX, with subsequent elimination of P_i to form oxazoline. This would explain the ATP requirement and is a speculation ultimately testable with ^{18}O-label in the Gly-Ser carbonyl oxygen. It is of note that the initial oxyanion cyclic adduct from Gly-Ser (or from Gly-Cys) is probably an intermediate common not only to the peptide-derived heterocyclic natural products but also in the pathways of protein autoproteolysis (*31*, *32*) and protein self-splicing reactions (*33*). Residues Ser, Cys, or Thr are present at both splice junction sites of such proteins. Thus, as shown in Fig. 6B, net O-protonation routes the initial cyclic adduct toward five-ring heterocycle formation, whereas N-protonation sets the adduct up for C–N bond cleavage in net peptide bond fragmentation. The oxoester product can hydrolyze by means of acyl transfer to water in the autoproteolysis sequence, typical of sonic hedgehog (a Gly-Cys peptide bond is cleaved) (*32*) or the proteosome precursors (a Gly-Thr peptide bond is cleaved) (*31*), or the product can undergo acyl transfer to an internal Ser or Cys side chain in the self-splicing sequences, for example, in RecA (*34*), Vent DNA polymerase (*35*), and TFP1 (*36*). Thus, the Gly-Ser (Gly-Cys) cyclization route may be rather ancient biochemistry with N-protonation as the default pathway, whereas routing of flux by O-protonation may require specific protein catalysis (for example, McbB or -D).

Several natural products, including thiostrepton, thiangazole, and patellamide (Fig. 1), stop at the dihydroaromatic five-membered thiazoline or oxazoline ring stage, presumably because of kinetic release before aromatization [which is also the case apparently for biogenesis of phleomycin, a thiazoline precursor to bleomycin (*37*)] or because the biosynthetic enzymes lack a terminal dehydrogenase activity. A priori, we reasoned the loss of two hydrogens and two electrons would most likely be a proton/hydride desaturation and that a flavoprotein desaturase was a catalytic entity to anticipate on the basis of precedents for acyl coenzyme A desaturase (*38*), dihydroorate dehydrogenase (*39*), MurB (*40*), and proline dehydrogenase (*41*), all flavoenzymes. Indeed, our finding that McbC purifies with one equivalent of flavin mononucleotide (FMN) makes it a likely terminal desaturase, predictively funneling the electrons removed from the β carbon of the oxazoline as a hydride ion and then passing them on to O_2 as cosubstrate for E·$FMNH_2$ reoxidations, explaining the requirement for O_2 and balancing the redox stoichiometry for each ring formed. We do not yet know for the eight ring–forming His_6-McbA or even in the two ring–forming McbA(1–46) the kinetic regioselectivity (that is, Ser before Cys as proposed in Fig. 6A) for ring formation or desaturation.

In sum, the ability to purify the McbB-, McbC-, and McbD-containing *E. coli* MccB17 synthase and the initial findings on mechanism, propeptide recognition, and cofactor requirements set the stage for structure and function studies to analyze the individual roles of these three proteins and their counterparts in other such heterocycle biosynthetic enzymes and to define the rules for recognition of peptide substrates.

REFERENCES AND NOTES

1. J. R. Lewis, *Nat. Prod. Rep.* **12**, 135 (1995).
2. W. Wu, D. E. Vanderwall, J. Stubbe, J. W. Kozarich, C. J. Turner, *J. Am. Chem. Soc.* **116**, 10843 (1994); R. A. Manderville, J. F. Ellena, S. M. Hecht, *ibid.*, p. 10851.
3. E. Jurkiewicz *et al.*, *Antivir. Chem. Chemother.* **3**, 189 (1992); R. Jansen *et al.*, *Liebigs Ann. Chem.* **1992**, 357 (1992).

4. C. M. Ireland, A. R. J. Durso, R. A. Newman, M. P. Hacker, *J. Org. Chem.* **47**, 1807 (1982); A. B. Williams and R. S. Jacobs, *Cancer Lett.* **71**, 97 (1993).
5. H. G. Floss and J. M. Beale, *Angew. Chem. Int. Ed. Engl.* **28**, 146 (1989).
6. C. Freeman *et al.*, *Diagn. Microbiol. Infect. Dis.* **21**, 47 (1995); A. Barry and P. Fuchs, *Antimicrob. Agents Chemother.* **39**, 238 (1995).
7. J. L. Vizán, C. Hernández-Chico, I. del Castillo, F. Moreno, *EMBO J.* **10**, 467 (1991).
8. A. Bayer, S. Freund, G. Nicholson, G. Jung, *Angew. Chem. Int. Ed. Engl.* **32**, 1336 (1993); P. Yorgey *et al.*, *Proc. Natl. Acad. Sci. U.S.A.* **91**, 4519 (1994); A. Bayer, S. Freund, G. Jung, *Eur. J. Biochem.* **234**, 414 (1995).
9. J. L. San Millán, R. Kolter, F. Moreno, *J. Bacteriol.* **163**, 1016 (1985).
10. J. L. San Millán, C. Hernández-Chico, P. Pereda, F. Moreno, *ibid.*, p. 275.
11. J. Davagnino, M. Herrero, D. Furlong, F. Moreno, R. Kolter, *ibid.*, **1**, 230 (1986).
12. M. Garrido, M. Herrero, R. Kolter, F. Moreno, *EMBO J.* **7**, 1853 (1988).
13. O. Genilloud, F. Moreno, R. Kolter, *J. Bacteriol.* **171**, 1126 (1989).
14. P. Yorgey, J. Davagnino, R. Kolter, *Mol. Microbiol.* **9**, 897 (1993).
15. L. L. Madison, E. I. Vivas, Y.-M. Li, C. T. Walsh, R. Kolter, *ibid.*, in press.
16. Plasmid pLarA-15b was generated by inserting the *mcbA* gene that was amplified by polymerase chain reaction (PCR) from pPY113 into the expression vector pET15b (Nde I–Bam HI sites) (Novagen). His_6-McbA expression was induced in BL21(DE3)(pLarA-15b) cells and purified by Ni^{2+}-chelate chromatography. The His_6 tag adds 20 aa to the NH_2-terminus of McbA. Mass spectrometry and amino acid analysis indicated that the first Met was removed.
17. Aminoethyl bithiazole carboxylic acid was cross-linked to BSA by disuccinimidyl suberate through primary amines. Protein immunoblot analysis showed that the cross-linked sample was recognized by anti-MccB17, whereas control samples (BSA alone and BSA plus disuccinimidyl suberate) were not.
18. Y.-M. Li, J. C. Milne, L. L. Madison, R. Kolter, C. T. Walsh, data not shown.
19. The plasmids pChenB, pChenC, and pChenD contain gene-disrupting insertions [mini Tn10 kanamycin resistance (*kan*^{r})] in *mcbB*, *mcbC*, and *mcbD* of pCID909 (*12*), respectively (T. Chen and R. Kolter, unpublished results). The parent pCID909 and knockout plasmids pChenB, pChenC, and pChenD were transformed into ZK4 cells [L. Gilson, H. K. Mahanty, R. Kolter, *J. Bacteriol.* **169**, 2466 (1987)], and the cellular extracts were used for an in vitro assay as described in Fig. 3B.
20. ZK4(pPY113) containing the seven genes *mcbA* through *mcbG* cloned into pBR322 (*10*) was used for MccB17 synthase production.
21. Protein amounts were determined with the Bradford reagent (Bio-Rad). McbA–β-Gal was used as substrate of MccB17 synthase. A time course of the modification was monitored by protein immunoblot and quantitated by the NIH-Image program. A point in the linear range was used to calculate the specific activity. The uncalibrated optical density was used for the area determination in the same blot.
22. The k_{cat} for McbA(1–46) was estimated from the linear portion of rate plots as in Fig. 3B. Conversion of the absorbance units in the immunoblot to picomoles of bisheterocycle product was obtained from endpoint absorbance where MS analysis revealed only bisheterocycle product.
23. J. C. A. Bardwell and E. A. Craig, *Proc. Natl. Acad. Sci. U.S.A.* **84**, 5177 (1987). We hypothesized that HtpG could possibly function as a chaperone in McbA recognition, but subsequent analysis of an *htpG* knockout strain of *E. coli* (MC4100 Δ*htpG*) indicated no effect on MccB17 production assessed by a bioassay (*9*) and at most a 50% decrease in the rate of posttranslational modification of McbA–β-Gal in vitro (*18*). Therefore, the role of HtpG in MccB17 maturation remains uncertain. MC4100 Δ*htpG* was constructed by P_1 transduction of *zba-315::kan*, Δ*htpG::lacZ* from JCB42 [J. C. A. Bardwell and E. A. Craig, *J. Bacteriol.* **170**, 2977 (1988)]. The *htpG* knockout strain MC4100 Δ*htpG* and control strain MC4100 were transformed with plasmid pPY113. These strains were assayed as described in Fig. 3B except that the McbA–β-Gal concentration was 30 μM.
24. Plasmid pLarB-11d was generated by insertion of the *mcbB* gene into the expression vector pET-11d-CKIIβα (Nde I–Bam HI sites) [Y. Shi, E. D. Brown, C. T. Walsh, *Proc. Natl. Acad. Sci. U.S.A.* **91**, 2767 (1994)]. Plasmids pLarC-15b and pLarD-15b were constructed by cloning *mcbC* and *mcbD* into the expression vector pET-15b (Nde I–Bam HI sites), respectively. All three genes were amplified by PCR from pPY113 with the specific primers with restriction sites (Nde I or Bam HI). McbB was purified from DE3(BL21)(pLarB-11d) by five-step purification: Q-Sepharose, ammonium sulfate precipitation, gel filtration, Phenyl-Sepharose, and MonoQ. His_6-McbC was purified from a strain of DE3(BL21)pLysS(pLarC-15b) by Ni^{2+}-chelate chromatography. His_6-McbD was purified from inclusion bodies of DE3(BL21) pLysS(pLarD-15b) by affinity chromatography and SDS-PAGE.
25. Attempts to effect modification of McbA(27–69) or Mcb(27–46) by adding McbA(1–26) in trans have not resulted in heterocycle formation. Combinations of three concentrations (9.6, 2.4, and 0.6 μM) of McbA(1–26) and four concentrations (135, 24, 85, and 2.1 μM) of McbA(27–69) were used to test the two peptides in trans for heterocycle formation. The assay conditions were as described in Fig. 5A. The reactions at 0 and 120 min were stopped and analyzed by protein immunoblot.
26. M. J. Jorgensen *et al.*, *Cell* **48**, 185 (1987); B. R. Hubbard *et al.*, *J. Biol. Chem.* **264**, 14145 (1989).
27. K. Siegers, S. Heinzmann, K.-D. Entian, *J. Biol. Chem.* **271**, 12294 (1996).
28. In vivo data to be presented elsewhere (*15*) on the McbA–β-Gal fusion construct further confirms that the (1–26) propeptide region is a major recognition determinant for MccB17 synthase.
29. Reaction components were degassed separately in reactivials (Pierce) fitted with silicon–teflon septa on a vacuum line by repeated evacuation and backfilling with argon (for anaerobic reactions) or air (for control reactions) (10 times). The vials were then incubated on ice for 30 min, and the degassing procedure was repeated two more times. Anaerobic modification reactions were carried out in a controlled atmosphere glove box (Model 50004; Labconco) that had been evacuated and backfilled with argon five times, and control reactions were carried out on the bench top. The modification reactions were carried out essentially as described above for Mcb(1–46). To assess the level of oxygen remaining after the degassing procedure, the activity of glucose oxidase was determined. Glucose oxidase catalyzes the oxidation of β-D-glucose using O_2 as the hydrogen acceptor. Glucose oxidase activity was determined with the glucose oxidase–peroxidase–*o*-dianisidine assay system [H. U. Bergmeyer, *Methods of Enzymatic Analysis* (Academic Press, New York, 1974), vol. 1, p. 457]. The reaction mix contained 0.04 units of glucose oxidase (Calbiochem), 0.4 units of horseradish peroxidase (Calbiochem), 0.37 M β-D-glucose, *o*-dianisidine (0.4 mg/ml) (Sigma), and 0.1 M sodium phosphate (pH 7.0). The reaction was initiated by adding glucose oxidase to the reacation mix. Samples were removed at 4, 8, 12, and 16 min, the reaction was quenched with HCl, and the absorbance at 460 nm was then determined.
30. The optical spectrum of purified McbC indicated the presence of a flavin moiety. The flavin was released from the enzyme by boiling for 15 min. The denatured protein was removed by centrifugation, and the flavin was identified by HPLC analysis (Vydac C18 protein–peptide column) with a gradient of methanol (10 to 40% in 60 min) in 0.1 M potassium phosphate (pH 5.3).
31. P. Zwickl, J. Kleinz, W. Baumeister, *Nature Struct. Biol.* **5**, 765 (1994).
32. J. J. Lee *et al.*, *Science* **266**, 1528 (1994); J. A. Porter *et al.*, *Nature* **374**, 363 (1995).
33. M.-Q. Xu, M. W. Southworth, F. B. Mersha, L. J. Hornstra, F. B. Perler, *Cell* **75**, 1371 (1993); M.-Q. Xu *et al.*, *EMBO J.* **23**, 5517 (1994); N. D. Clarke, *Proc. Natl. Acad. Sci. U.S.A.* **91**, 11084 (1994); A. A. Cooper and T. H. Stevens, *Trends Biochem. Sci.* **20**, 351 (1995).
34. E. O. Davis, P. J. Jenner, P. C. Brooks, M. J. Colston, S. G. Sedgwick, *Cell* **71**, 201 (1992).
35. R. A. Hodges, F. B. Perler, C. J. Noren, W. E. Jack, *Nucleic Acids Res.* **20**, 6135 (1992).
36. A. A. Cooper, Y. J. Chen, M. A. Lindorfer, T. H. Stevens, *EMBO J.* **12**, 2575 (1993).
37. T. Takita *et al.*, *J. Antibiotics* **25**, 197 (1972).
38. F. J. Ruzicka and H. Beinert, *J. Biol. Chem.* **252**, 8440 (1977).
39. R. A. J. Pascal, N. L. Trang, A. Cerami, C. Walsh, *Biochemistry* **22**, 171 (1983).
40. T. E. Benson, M. J. L., M. A. C., F. A. Etzkorn, C. T. Walsh, *ibid.* **32**, 2024 (1993).
41. R. C. Scarpulla and R. L. Soffer, *J. Biol. Chem.* **153**, 5997 (1978).
42. The Sal I–Xmn I fragment of *mcbA* was used to generate an in-frame fusion with β-Gal at the 65th codon of *mcbA*, creating the plasmid pPY116 (*15*). McbA–β-Gal was purified from the strain ZK4(pPY116) with an aminobenzyl 1-thio-β-D-galactopyranoside-agarose column (Sigma).
43. All four peptides were purified by HPLC [Bio-Rad Preparative C18 column, with solvent A: 0.1% trifluoroacetic acid (TFA) in water, and solvent B: 0.1% TFA in acetonitrile] and the structure confirmed by mass spectrometry. The concentration of the peptides was determined by amino acid analysis.
44. The ZK4(pPY113) strain was used for purification of MccB17 synthase. An overnight culture grown in LB media containing ampicillin (Amp) was diluted 500-fold in M63 medium containing Amp and grown at 37°C for 20 to 24 hours. The cells were pelleted by centrifugation (5000*g*) and lysed with a French pressure cell. The supernatant after 105,000*g* centrifugation was used for purification by phenyl-Sepharose, DEAE-Sepharose, Sephacryl S-200, and MonoQ (Pharmacia). The activity was monitored by protein immunoblot analysis as described in Fig. 3, with McbA–β-Gal as a substrate.
45. Polyclonal rabbit antibodies to each protein were generated by East-Acres Biologicals. Protein immunoblot analysis shows that the antisera specifically recognize their antigen and do not cross-react with other proteins (*18*). The immunocomplexes were washed with buffer [50 mM tris-HCl (pH 7.5), 100 mM KCl, 4 mM $MgCl_2$, 2 mM $CaCl_2$] four times and collected by centrifugation. SDS sample buffer was added to the complex, and the supernatants were subjected to protein immunoblot analysis.
46. Reaction mixtures consisted of 7 μM McbA(1–46), 50 mM tris-HCl (pH 7.5), 50 mM KCl, 2 mM $MgCl_2$, 1 mM $CaCl_2$, 1 mM ATP, 1 mM dithiothreitol, and purified MccB17 synthase (0.24 mg/ml). The reactions were carried out at 37°C and stopped by injection onto HPLC (Vydac C18 column, 300 Å, solvent A: 0.1% TFA in water, and solvent B: 0.09% TFA in acetonitrile). McbA(1–46) was eluted around 33% solvent B. The 0- and 45-min reaction mixtures showed the same elution patterns, a peak at 33% solvent B and other protein peaks after >45% solvent B. HPLC fractions were analyzed by protein immunoblot with anti-MccB17 and only the peak (33% solvent B) for the 45-min reaction was antibody-positive (*18*).

47. We thank C. E. Dahl of the Department of Biological Chemistry and Molecular Pharmacology of the Biopolymers Facility for synthesis of the microcin peptides; I. Jenson and M. Obenauer of Howard Hughes Medical Institute Research Laboratory for NH_2-terminal sequencing, amino acid analysis, and MS analysis; S. Hecht (University of Virginia) for aminoethyl bithiazole carboxylic acid; M. Bollinger (Pennsylvania State University) and S. Fisher and D. McCafferty of this laboratory for their help and suggestions regarding the anaerobic reactions. We also thank other members of the C.T.W. laboratory for suggestions concerning this manuscript. Supported by NIH grant GM20011 (C.T.W.) and NSF grant MCB9207323 (R.K.). J.C.M. is supported by a postdoctoral fellowship (grant PF4332) from the American Cancer Society, and L.L.M. is supported by NIH training grants 5T32GM07306-19 and 5T32AI07410-03.

19 July 1996; accepted 6 September 1996